To the Graduate Council:

I am submitting herewith a thesis written by George Russell McNutt III entitled "A Study of Cracks in a Three-Dimensional Finite Medium Employing the Boundary Element Method." I have examined the final copy of this thesis for form and content and recommend that it be accepted in partial fulfillment of the requirements for the degree of Master of Science, with a major in Engineering Science.

J.A.M. Boulet

J.A.M. Boulet, Major Professor

We have read this thesis and recommend its acceptance:

Raymond A. King

John D. Landes

Accepted for the Council:

C.W. Minkel

Associate Vice Chancellor and Dean of The Graduate School

STATEMENT OF PERMISSION TO USE

In presenting this thesis in partial fulfillment of the requirements for a Masters degree at The University of Tennessee, Knoxville, I agree that the Library shall make it available to borrowers under the rules of the Library. Brief quotations from this thesis are allowed without special permission, provided that accurate acknowledgment of the source is made.

Permission for extensive quotation from or reproduction of this thesis may be granted by my major professor, or in his absence, by the Head of Interlibrary Services when, in the opinion of either, the proposed use of the material is for scholarly purposes. Any copying or use of the material in this thesis for financial gain shall not be allowed without my written permission.

Signature [illegible]

Date December 20, 1992

A Study of Cracks in a Three-Dimensional Finite Medium Employing the Boundary Element Method

A Thesis
Presented for the
Master of Science
Degree
The University of Tennessee, Knoxville

G. Russell McNutt III

December, 1992

DEDICATION

This thesis is dedicated to my late grandfather
Mr. Sam Kinser whose life and personality inspired and influenced me.

ACKNOWLEDGMENTS

I would like to thank my major professor, Dr. J.A.M. Boulet for his guidance and help over the past two and a half years. I would also like to thank my other committee members, Dr. Raymond D. Krieg and Dr. John D. Landes for their contributions. I would like to thank Dr. T.A. Cruse and Southwest Research Institute for the use of BINTEQ and DDID. I would especially like to thank Dr. Mike Keene and Cathleen Wynn for their help with my writing. Finally, I would like to thank Karen Hamilton for her support and love when things did not look good.

ABSTRACT

The work presented herein is a method for analyzing cracked, finite, linearly elastic bodies. A mathematical model for the behavior of cracks in a finite medium is presented that is capable of handling any shaped crack in a given domain. The model employs the boundary element method using Somigliana's displacement identity and a traction boundary integral equation. The model was tested using a circular crack embedded inside a circular cylinder subjected to axial tension. For infinitely long cylinders of various radii, results obtained from the method agreed with the analytical solution. For cylinders of finite length, the model gave results that are qualitatively correct. The significance of the model is that it has the potential of modeling cracks with irregular shapes where interference is possible due to crack face closure. It is concluded that the method is capable of accurately predicting the behavior of embedded cracks in a finite body and has the potential for handling crack-face interference and calculation of stress intensity factors.

TABLE OF CONTENTS

Chapter		Page
1	**Introduction**	1
2	**Problem Statement**	4
3	**Methodology**	12
4	**Results**	18
5	**Future Work**	32
6	**Conclusions**	35
	Bibliography	37
	Appendix	40
	Vita	42

LIST OF FIGURES

Figure Page

1. Cracked body showing location of crack surfaces and outer boundary.....5
2. Relationship between a source point and the field points located on a boundary of area dA.....7
3. Flow chart of codes showing input files read and output created.....17
4. Cylinder geometry showing crack orientation, loading, and coordinate system used.....19
5. Refined and coarse mesh nodes.....21
6. Plot of theoretical crack center displacement and center displacement as calculated by BRIDGE for both meshes.....22
7. Deformed mesh for the $r = 2.5$ inch cylinder showing axisymmetry of results.....24
8. Comparison of BRIDGE results along a radius with an ellipse showing elliptical shape of the deformed crack inside a cylinder of radius 2.5 inch.....25
9. Plot of BRIDGE results along a radius with an ellipse showing elliptical behavior of a crack inside a cylinder of radius 4 inches.....26
10. Comparison of crack center displacement vs. cylinder half-height for a 4 in. radius cylinder and a one inch radius crack.....27

11. Comparison of crack center displacement vs. cylinder half-height for a 2.5 inch radius cylinder and one inch radius crack..28
12. Plot of results for cylinder of 50 inch half-height and radius of 2.5 inches showing axisymmetry of results..................30
13. Comparison of BRIDGE results along a radius and ellipse showing elliptical behavior of a crack inside a cylinder of radius 2.5 inches..31
14. Two-dimensional representation of a virtual crack extension..34

CHAPTER 1

INTRODUCTION

The field of fracture mechanics is devoted to exploring how cracks affect the probability of failure in structures. This exploration requires an understanding of crack behavior. One of the most commonly used measures of failure probability is the stress intensity factor for the stress field around the edge of the crack. For linear elastic fracture mechanics, principles of elasticity are used first to calculate stresses or displacements, and then to calculate stress intensity factors from these results. Three basic methods are used in calculating elasticity solutions: theoretical, experimental, and numerical. Theoretical analysis yields exact values. Much effort has been devoted to solving different crack cases using a wide variety of theoretical approaches. Those cases that have been solved have been tabulated in handbooks and do not require further study. There are, however, many cases that are not solvable by theoretical methods. Experimental methods also have drawbacks because accurate measuring of cracks is essential, and current technology limits the accuracy of crack measurement. The numerical method is the most popular because it can be extended to include cases where the analytical solution would be extremely difficult, if not impossible, to obtain. Two kinds of numerical method used are finite element methods (FEM) and boundary integral equation (BIE) methods. The FEM has the disadvantage of having large systems of simultaneous equations with many interior points needed to model the problem, while the BIE method needs points only on the boundaries.

The BIE method is derived from Betti's reciprocal work theorem

$$\int_V \sigma_{ij}^1 \varepsilon_{ij}^2 \delta V = \int_V \sigma_{ij}^2 \, \varepsilon_{ij}^1 \delta V \tag{1.1}$$

from which Somigliana formulated a displacement identity for linear elasticity. This equation has been found to be useful in elasticity problems except where the stress field contains discontinuities. Within the BIE method, there have been several approaches to modeling of cracks. The first was to model the crack as two separate surfaces in contact with each other and to constrain the surfaces to simulate the crack (Cruse 1988). Because elements connecting the crack and exterior surfaces are required, this method has proven to be inaccurate and inconvenient. Another method used is a Green's function approach (Cruse 1988). This is an accurate method but is only applicable for two-dimensional problems. The third method, the displacement discontinuity method, accommodates a crack by using both Somigliana's displacement identity and a traction boundary integral. This method is still under development and is the method used in what follows.

Until recently, most three-dimensional crack simulations have used special geometries where the problem could be worked by symmetry (Cruse 1974). This allowed the domain to be simply connected. Other methods model a crack in an infinite medium. Cruse and Novati (Cruse 1990) developed a method for analyzing a general three-dimensional crack in an infinite medium without needing any elements outside the crack surface. The only methods for analyzing embedded three-dimensional cracks in a finite medium involve solving a finite, uncracked domain and then using an iterative method to solve for the displacements of a crack in an infinite domain. There is no previously published work modeling a three-dimensional crack in a finite body where the exterior and crack surfaces were solved together without connecting the regions. Nor has there been any published work modeling a generally shaped crack where the surfaces are not smooth. This means that crack geometries in which the surfaces may interact at some point other than the edges have not been modeled. The method discussed herein models a three-dimensional crack in a finite domain using the displacement discontinuity method and is capable of handling situations where crack-face interference may result.

CHAPTER 2

PROBLEM STATEMENT

In the standard boundary element approach, the governing equation for a cracked body (Figure 1) is given by Somigliana's displacement identity

$$
\begin{aligned}
u_i = \int_S U_{ij}\, t_j\, dS + \int_{\Gamma^+} U_{ij} t_j\, dS + \int_{\Gamma^-} U_{ij} t_j\, dS \\
- \int_S T_{ij}\, u_j\, dS - \int_{\Gamma^+} T_{ij} u_j\, dS - \int_{\Gamma^-} T_{ij}\, u_j\, dS
\end{aligned}
\qquad (2.1)
$$

where

u_i is the displacement vector of any point,

t_j is the traction vector on the outer surface,

u_j is the displacement vector for a point on a surface,

S is the external boundary of the region,

Γ^+ is the upper surface of the crack, and

Γ^- is the lower surface of the crack.

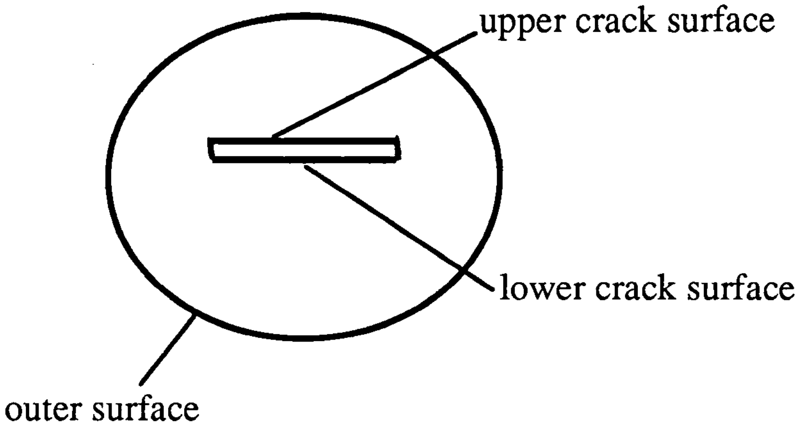

Figure 1. Cracked body showing location of crack surfaces and outer boundary.

The tensors T_{ij} andU_{ij} in (2.1) are

$$T_{ij} = \frac{-\frac{\partial r}{\partial n}\left[(1-2\nu)\delta_{ij} + 3r_{,i}\,r_{,j}\right] - (1-2\nu)\left[n_j\,r_{,i} - n_i\,r_{,j}\right]}{8\pi(1-\nu)r^2} \qquad (2.2)$$

and

$$U_{ij} = \frac{(3-4\nu)\delta_{ij} + r_{,i}\,r_{,j}}{16\pi\mu(1-\nu)r} \qquad (2.3)$$

where

ν is Poisson's ratio,

δ_{ij} is the Kronecker delta,

n_i is the unit vector normal to the surface (see Figure 2),

r is the distance between the point at which (2.1) is being evaluated (source point) and the current integration point (field point),

$r_{,i} = \dfrac{\partial r}{\partial x_i}$, and

$\dfrac{\partial r}{\partial n} = r_{,i}\,n_i.$

This identity, however, is not useful for finding the displacements of the crack surface because the tractions on the two crack surfaces are self-equilibrating and the integrals over the crack boundaries cancel out. The resulting system of equations does not provide a unique solution because any self-equilibrating load on a crack will result in the same solution. To find the behavior of the crack surface, a new formulation is needed. Instead of using crack face displacements, the *difference* in crack face displacements (displacement discontinuities) is used.

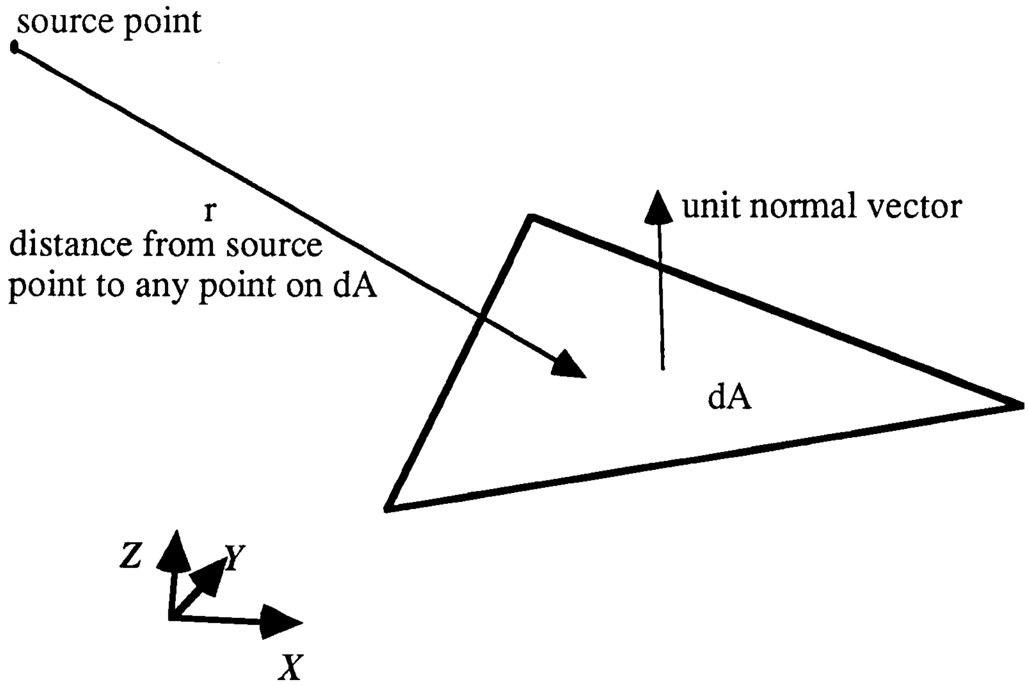

Figure 2. Relationship between a source point and the field points located on a boundary of area dA.

From this approach, Somigliana's identity for a cracked body is

$$u_i = \int_S U_{ij}\, t_j dS - \int_\Gamma T_{ij} \Delta u_j d\Gamma - \int_S T_{ij} u_j dS \tag{2.4}$$

where Γ is the crack surface,

$$\Delta u_j = u_j^+ - u_j^- \tag{2.5}$$

and u_j^+ and u_j^- are displacements at the field point on Γ^+ and Γ^-, respectively. For (2.4), the second term is a combination of the last two terms in (2.1) using (2.5). The second and third terms of (2.1) cancel out and are not present in (2.4).

By discretizing the boundary into discrete boundary elements, (2.4) can be transformed into a series of linear algebraic equations. Each algebraic equation is a discretized representation of (2.4) for a point on the boundary. Each boundary point for which (2.4) is written is called a source point. As the integrals are evaluated, the source points remain fixed while the integration point, or field point, moves over the boundary of the body. In practice, the integrals are evaluated numerically so that only a finite number of field points is used. The result is an equation for each source point with contributions from all field points. Linear triangular elements are used in the method discussed below with the field points (nodes) being the triangle vertices. The discretized form of (2.4) can be expressed as

$$[A]\{u_s\}+[E]\{\Delta u_\Gamma\}=[B]\{t_s\} \tag{2.6}$$

where

$[A]$, $[E]$, and $[B]$ are computed from the geometry and material properties given,

$\{u_s\}$ are the displacement components at the nodes of S,

$\{t_s\}$ are the nodal traction components on S, and

$\{\Delta u_\Gamma\}$ are the nodal displacement discontinuity components on Γ.

In practice, (2.4) is written once for each node on S. Thus each node, in turn, plays the role of source point while all nodes are the field points. It follows that the number of rows in (2.6) is equal to the size of $\{u_s\}$. But because the total number of unknowns is the sum of the orders of $\{u_s\}$ + $\{\Delta u_\Gamma\}$, the resulting system of equations has more unknowns than equations. This also means that the matrix $[E]$ will be a rectangular matrix with n rows and m columns where n is the number of displacements in $\{u_s\}$ and m is the number of displacement discontinuities in $\{\Delta u_\Gamma\}$.

The matrices $[A]$ and $[B]$ in (2.6) are n by n matrices. For cases where there is no crack present, the integral over Γ in (2.2) drops out and the matrix $[E]$ in (2.6) vanishes. The resulting system is square and can be solved by standard means. BINTEQ is a boundary element code developed by Cruse and Cardinal (Cruse 1969) that analyzes an uncracked domain in this manner. The source points and the field points in BINTEQ are the nodes of each element.

To solve for $\{u_s\}$ and $\{\Delta u_\Gamma\}$ in (2.6), additional equations are required. These equations are provided by analyzing the cracked domain using a traction boundary integral equation, instead of Somigliana's displacement identity. For a cracked domain, the traction boundary integral equation is

$$\sigma_{i3} = \int_S U^{\sigma}_{ki3} t_k dS - \int_S T^{\sigma}_{ki3} u_k dS - \int_\Gamma T^{\sigma}_{ki3} \Delta u_k d\Gamma \tag{2.7}$$

where σ_{i3} is the traction vector on Γ, and the tensors T^{σ}_{ki3} and U^{σ}_{ki3} are

$$\begin{aligned} T^{\sigma}_{kj3} = \frac{c\mu}{2\pi r^3}\Bigg\{ & 3\frac{\partial r}{\partial n}\Bigg[\delta_{j3} r_{,k} + \frac{\nu}{1-2\nu}\left(\delta_{k3} r_{,j} + \delta_{j3} r_{,k}\right) - \\ & \frac{5}{1-2\nu} r_{,j} r_{,k} r_{,3}\Bigg] + 3\nu \frac{\left(n_j r_{,3} r_{,k} + n_3 r_{,k} r_{,j}\right)}{1-2\nu} + \\ & 3n_k r_{,j} r_{,3} + n_3 r_{,j} r_{,k} + n_j \delta_{k3} - \frac{1-4\nu}{1-2\nu} n_k \delta_{j3} \Bigg\} \end{aligned} \tag{2.8}$$

and

$$U^{\sigma}_{ik3} = \frac{c}{4\pi r^2}\left(\delta_{ik} r_{,3} + \delta_{i3} r_{,k} - \delta_{k3} r_{,i} + \frac{3}{1-2\nu} r_{,i} r_{,k} r_{,3}\right) \tag{2.9}$$

Using discrete boundary elements, we write (2.7) once for each source point on Γ to produce

$$[G]\{u_s\} + [C]\{\Delta u_\Gamma\} = [F]\{t_s\} + [D]\{t_\Gamma\} \tag{2.10}$$

with $[G]$,$[C]$,$[F]$, and $[D]$ being computed from the given geometry and material constants and with $\{t_\Gamma\}$ being the vector of traction components on the crack faces. This system of equations, like (2.4), has more unknowns than equations, with the number of equations being on the order of $\{\Delta u_\Gamma\}$.

The matrices $[G]$ and $[F]$ are rectangular matrices with m rows and n columns where m and n represent the total number of displacement discontinuities in $\{\Delta u_\Gamma\}$ and displacements in $\{u_s\}$, respectively.

The matrices $[C]$ and $[D]$ are m by m. If the crack is in an infinite body, then matrices $[F]$ and $[G]$ vanish and the resulting system is square and solvable by standard means. DDID, a computer code developed by Cruse and Novati (Cruse 1990), performs such an analysis. DDID uses source points internal to each element and nodal field points.

For a finite cracked domain, (2.6) and (2.10) can be used together to form a square system of equations with an order equal to m plus n. The result is

$$\begin{bmatrix} [A] & [E] \\ [G] & [C] \end{bmatrix} \begin{Bmatrix} u_s \\ \Delta u_\Gamma \end{Bmatrix} = \begin{bmatrix} [B] & [0] \\ [F] & [D] \end{bmatrix} \begin{Bmatrix} t_s \\ t_\Gamma \end{Bmatrix} \tag{2.11}$$

where the matrices $[A]$, $[B]$, and $[C]$ are formed by DDID and BINTEQ. The remaining matrices $[D]$, $[E]$, $[F]$, and $[G]$ are formed herein by BRIDGE, an original computer code developed in support of this thesis.

CHAPTER 3

METHODOLOGY

Because the matrices $[A]$, $[C]$, $[B]$ [see (2.11)] are calculated by DDID and BINTEQ, the matrices $[D]$, $[E]$, $[F]$, and $[G]$ remain to be formed. This is done by numerical integration in a code called BRIDGE. For each of the remaining integrals in (2.4) and (2.7), the source points will be on one boundary and the field points will be on the other boundary. This means that the integrals will all be nonsingular and can be calculated in a straight-forward manner.

For the construction of $[E]$, the integral is

$$\int_{\Gamma} T_{ij} \Delta u_j \, d\Gamma \tag{3.1}$$

which is an integral over the (triangular) crack surface elements using the BINTEQ mesh source points. Because nodal values of the displacements and displacement discontinuities are used, the above integral can be simplified to

$$\int_{\Gamma} T_{ij} \Phi_{jk} \, d\Gamma \{\Delta u_k\} \tag{3.2}$$

where the Δu_j are nodal displacement discontinuities grouped by nodes and Φ_{jk} is an interpolation matrix. Because each boundary element has three nodes, each with three degrees of freedom, the above integral results in a 3 by 9 matrix for each element. The interpolation matrix is needed to express T_{ij} in terms of nodal displacement discontinuities. T_{ij} is integrated over the triangular element using oblique (area) coordinates (see appendix) and linearly interpolating between the nodes by

$$\int_{\Gamma} T_{ij}\, \Phi(\eta_k) d\Gamma \{\Delta u_k\} \tag{3.3}$$

where

η_k are the interpolation functions, and

$\{\Delta u_k\}$ is a vector with nine entries for each element.

For BINTEQ, the interpolation matrix is

$$\Phi(\eta_k) = \begin{bmatrix} \eta_1 & \eta_1 & \eta_1 & 0 & 0 & 0 & 0 & 0 & 0 \\ 0 & 0 & 0 & \eta_2 & \eta_2 & \eta_2 & 0 & 0 & 0 \\ 0 & 0 & 0 & 0 & 0 & 0 & \eta_3 & \eta_3 & \eta_3 \end{bmatrix} \tag{3.4}$$

and the interpolation matrix for DDID is

$$\Phi(\eta_k) = \begin{bmatrix} \eta_1 & 0 & 0 & \eta_2 & 0 & 0 & \eta_3 & 0 & 0 \\ 0 & \eta_1 & 0 & 0 & \eta_2 & 0 & 0 & \eta_3 & 0 \\ 0 & 0 & \eta_1 & 0 & 0 & \eta_2 & 0 & 0 & \eta_3 \end{bmatrix} \tag{3.5}$$

Both interpolation matrices are used in the BRIDGE code.

To perform the integrals, Gauss-Legendre quadrature is used. In this method, the integral is evaluated as

$$I = \int_0^1 \int_0^{1-\eta_2} f(\eta_1, \eta_2, \eta_3) d\eta_1 \, d\eta_2 \cong \frac{G}{2} \sum_{i=1}^{n} f\left(\eta_1^i, \eta_2^i, \eta_2^i\right) w_i \qquad (3.6)$$

where

G is twice the area of the triangle,

n is the order of the interpolation,

$f\left(\eta_1^i, \eta_2^i, \eta_3^i\right)$ is the integrand evaluated at integration point i, and

w_i are weight factors.

The weights and integration points are taken from (Brebbia 1984). The resulting equation for $[E]$ is

$$[E] = \frac{G}{2} \sum_{i=1}^{n} \sum_{j=1}^{3} T_{kj}\left(\eta_1^i, \eta_2^i, \eta_3^i\right) \, \Phi_{jm}\left(\eta_1^i, \eta_2^i, \eta_3^i\right) w_i \qquad (3.7)$$

where

$$T_{ij} = \frac{-\frac{\partial r}{\partial n}\left[(1-2\nu)\delta_{ij} + 3 r_{,i} \, r_{,j}\right] - (1-2\nu)\left[n_j \, r_{,i} - n_i \, r_{,j}\right]}{8\pi(1-\nu) r^2} \qquad (2.2)$$

ν is Poisson's ratio,

δ_{ij} is the Kronecker delta,

n_i is the unit normal vector,

r is the distance between the source point and the field point,

$r_{,i} = \frac{\partial r}{\partial x_i}$

$\frac{\partial r}{\partial n} = r_{,i} \, n_i$, and

η, Γ, and w are as before.

The calculation of $[F]$ follows similarly from the integral

$$\int_S U^{\sigma}_{ki3} t_k dS \tag{3.8}$$

which is an integration over the outer domain mesh with the source points in the crack mesh. This integral is evaluated numerically to give

$$[F] = \frac{G}{2} \sum_{j=1}^{n} \sum_{k=1}^{3} U^{\sigma}_{ik3}(\eta_1^j, \eta_2^j, \eta_3^j) \Phi_{km}\left(\eta_1^j, \eta_2^j, \eta_3^j\right) w_j \tag{3.9}$$

where the kernel is represented by

$$U^{\sigma}_{ik3} = \frac{c}{4\pi r^2}(\delta_{ik} r_{,3} + \delta_{i3} r_{,k} - \delta_{k3} r_{,i} + \frac{3}{1-2v} r_{,i} r_{,k} r_{,3}) \tag{2.9}$$

where

$$c = \frac{1-2v}{2(1-v)}$$

The formulation of $[G]$ from

$$\int_S T^{\sigma}_{ki3} u_k dS \tag{3.10}$$

yields

$$[G] = \frac{G}{2} \sum_{j=1}^{n} \sum_{i=1}^{3} T^{\sigma}_{ki3}(\eta_1^j, \eta_2^j, \eta_3^j) \Phi_{im}(\eta_1^j, \eta_2^j, \eta_3^j) w_j \tag{3.11}$$

The kernel T^{σ}_{ki3} is

$$T^{\sigma}_{kj3} = \frac{c\mu}{2\pi r^3}\left\{3\frac{\partial r}{\partial n}\left[\delta_{j3}\, r_{,k} + \frac{\nu}{1-2\nu}\left(\delta_{k3}\, r_{,j} + \delta_{j3}\, r_{,k}\right) - \frac{5}{1-2\nu} r_{,j}\, r_{,k}\, r_{,3}\right] + 3\nu\frac{\left(n_j\, r_{,3}\, r_{,k} + n_3\, r_{,k}\, r_{,j}\right)}{1-2\nu} + 3n_k\, r_{,j}\, r_{,3} + n_3\, r_{,j}\, r_{,k} + n_j\, \delta_{k3} - \frac{1-4\nu}{1-2\nu} n_k\, \delta_{j3}\right\} \tag{2.8}$$

The product of $[D]\{t_\Gamma\}$ is a vector whose values represent the negative of the tractions on the crack nodes. These values are calculated by determining the stress state of the crack nodes using BINTEQ. The tractions are then calculated from the stress state and the crack geometry. The matrices, $[D]$, $[E]$, $[F]$, and $[G]$, are assembled together with the matrices formed by DDID and BINTEQ to form (2.11). The resulting system is square and solvable by standard means. Figure 3 is a flow chart of how the codes fit together and what they calculate.

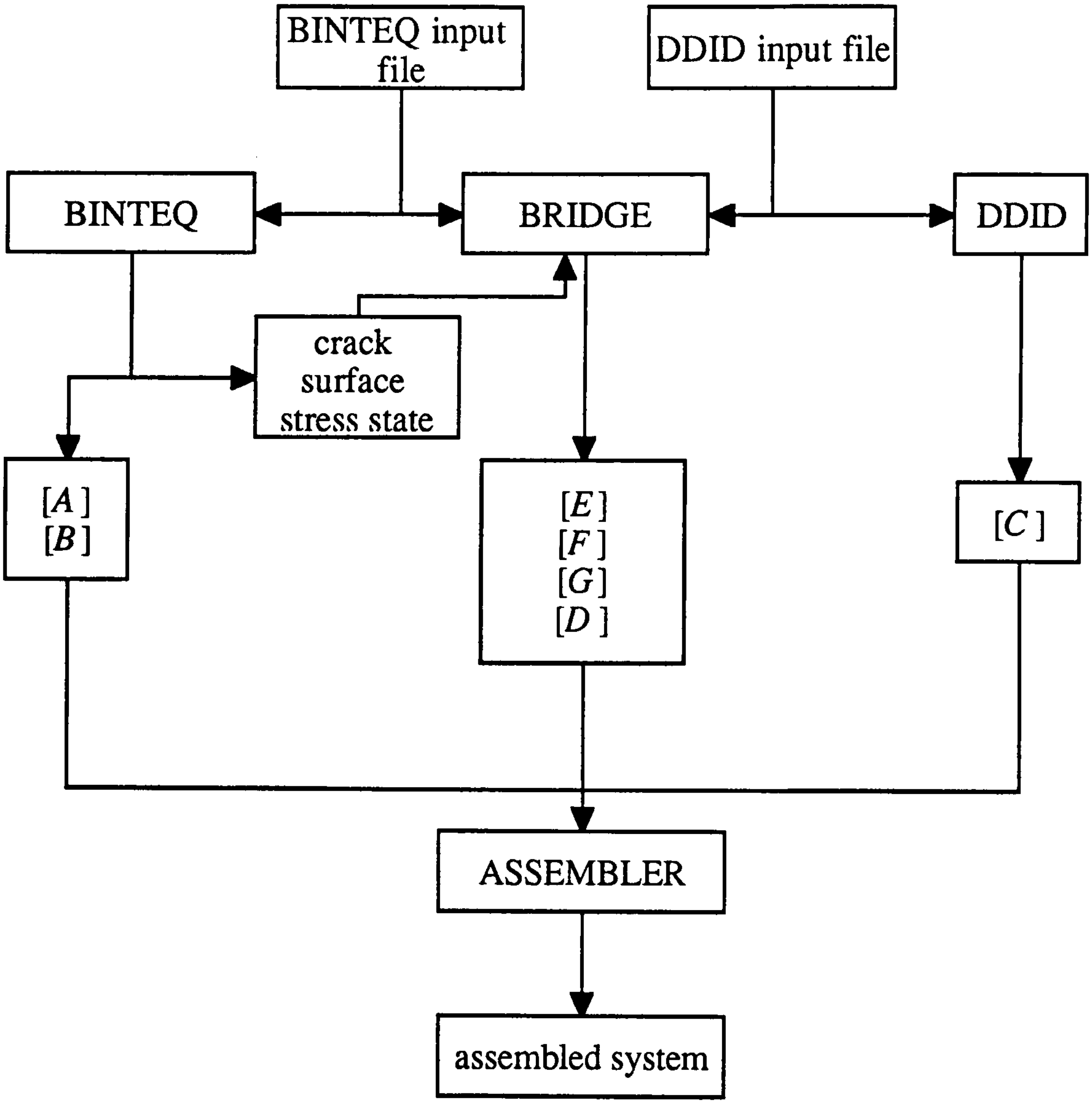

Figure 3. Flow chart of codes showing input files read and output created.

CHAPTER 4

RESULTS

Once the individual matrices have all been formed, they can be assembled to form

$$\begin{bmatrix} [A] & [E] \\ [G] & [C] \end{bmatrix} \begin{Bmatrix} u_s \\ \Delta u_\Gamma \end{Bmatrix} = \begin{bmatrix} [B] & [0] \\ [F] & [D] \end{bmatrix} \begin{Bmatrix} t_s \\ t_\Gamma \end{Bmatrix} \tag{2.11}$$

which is a system of linear algebraic equations that can be solved by standard means. To test the new method, a problem for which the theoretical result is known was selected.

The BRIDGE simulation was tested with a circular crack inside a cylinder. The geometry, loading, and coordinate frame are shown in Figure 4. For the case of an infinite cylinder with finite radius under uniaxial tension, the displacement at the center of the crack is (Tada 1985)

$$\delta = \frac{8(1-\nu^2)}{\pi E} \sigma a H\left(\frac{a}{b}\right) \tag{4.1}$$

where

δ is the opening at the center,

σ is the remote stress,

E is the modulus of elasticity,

a is the crack radius,

b is the radius of the cylinder, and

ν is as before.

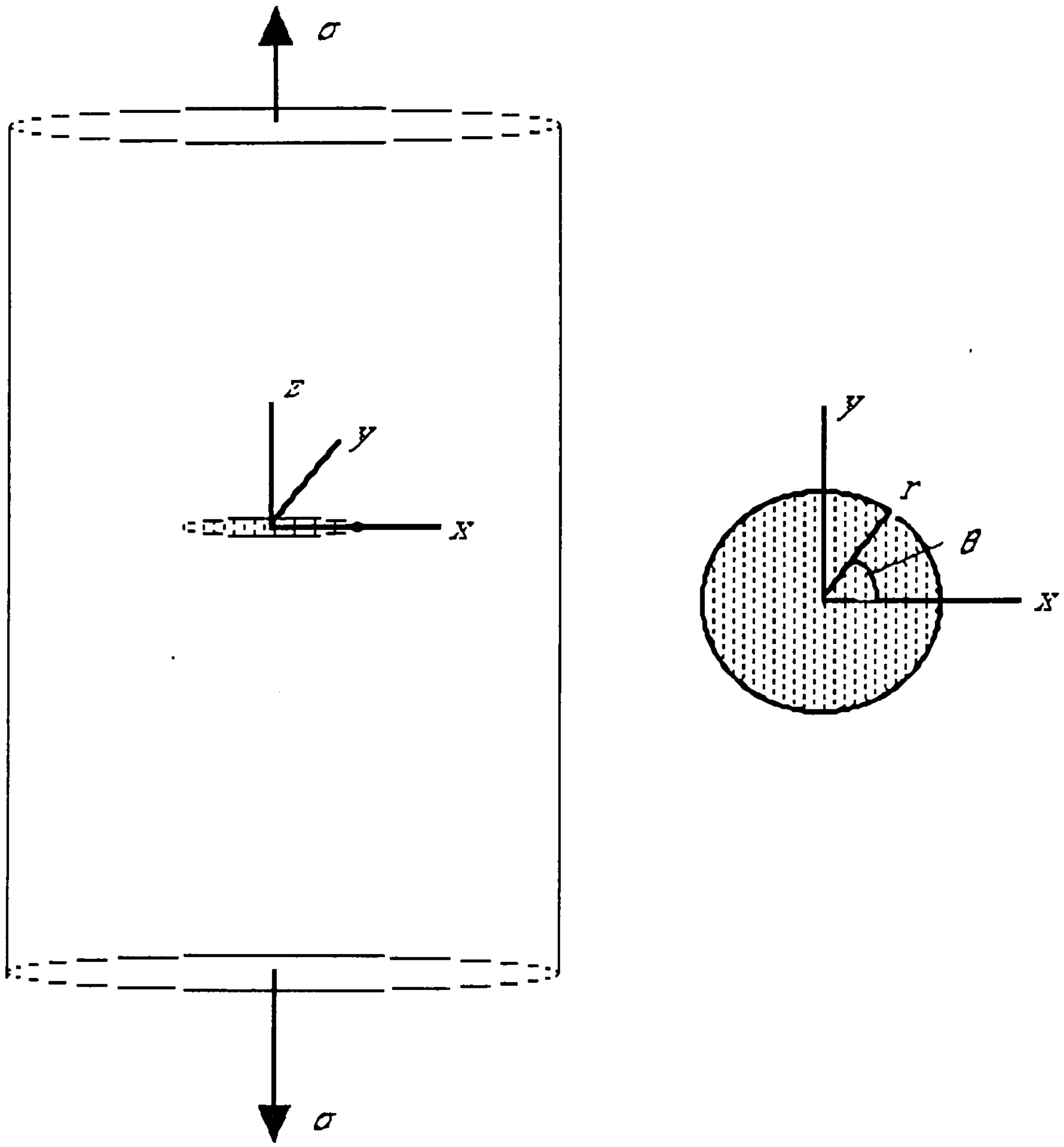

Figure 4. Cylinder geometry showing crack orientation, loading, and coordinate system used.

The function H is represented by

$$H\left(\frac{a}{b}\right)=\frac{b}{a}\, ln\left(\frac{1}{1-\dfrac{a}{b}}\right)\left[1-\frac{1}{2}\frac{a}{b}+0.34\left(\frac{a}{b}\right)^{3.5}\right] \tag{4.2}$$

For an infinite body, the function H goes to a value of 1.0.

The method was tested for various cylinder heights and radii. For the initial cases, the cylinder height was 1200 inches, the crack radius was one inch, and two different crack meshes were used. The meshes are shown in Figure 5.

Figure 6 shows a comparison of each case and the theoretical results for the displacement of the center of the crack. For each case, an elastic modulus of 10E+6 psi and a Poisson's ratio of 0.3 were used. An axial traction of 1000 psi was applied in the z-direction on the ends. The figure shows that the accuracy of the results is improved by using a finer crack mesh. In principle, the accuracy of the results could be improved by further mesh refinement. The results for the cylinder with a radius of 5 inches did not change significantly with the two crack meshes. This lack of change indicates that the results have converged to the limit of the code's ability. For this case, because the theoretical value is only one percent greater than that for a cylinder of infinite radius, the cylinder radius is essentially infinite. The DDID code was able to calculate the crack center displacement within 1% of the theoretical value; therefore the error is the result of the combination of the BRIDGE contributions and computer limitations.

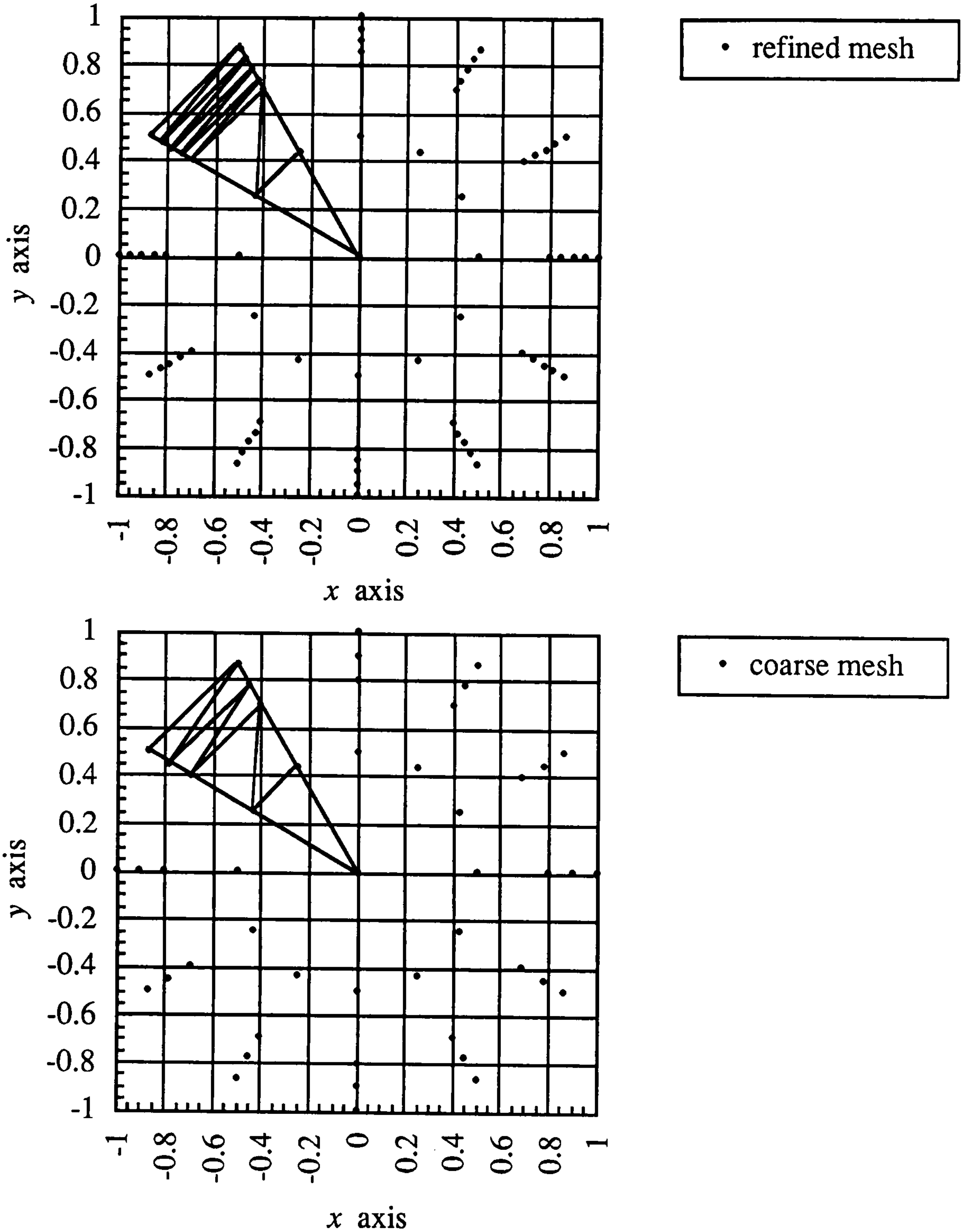

Figure 5. Refined and coarse mesh nodes (all dimensions in inches).

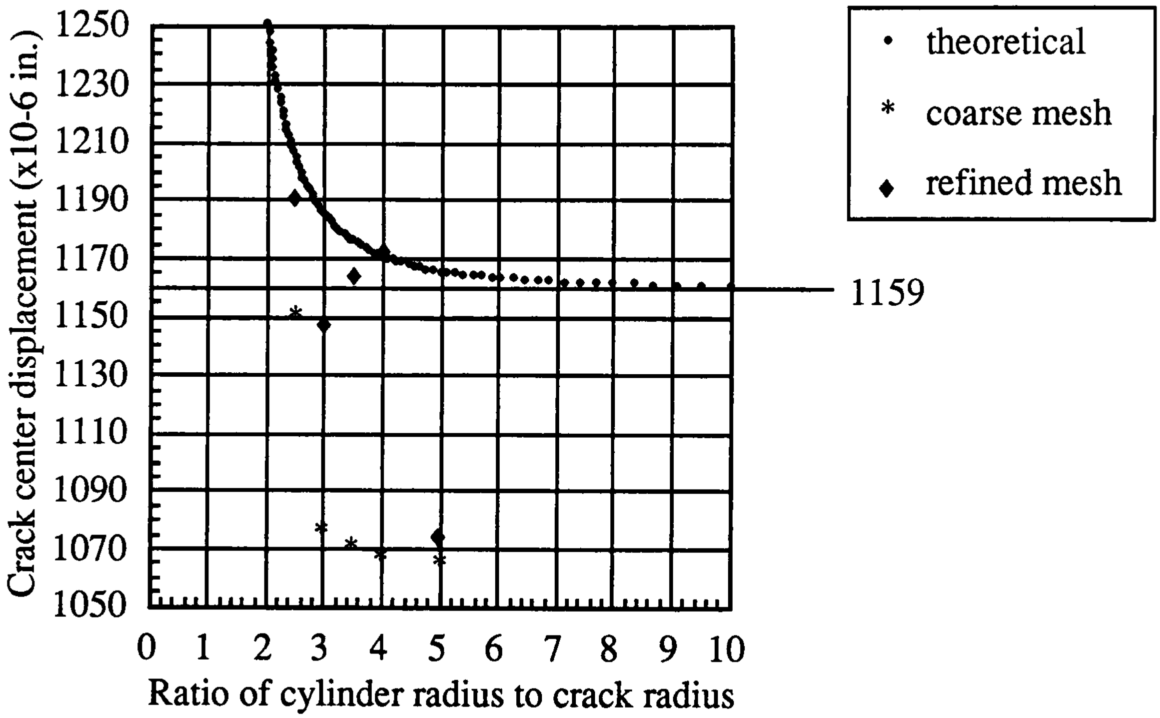

Figure 6. Plot of theoretical crack center displacement and center displacement as calculated by BRIDGE for both meshes.

Figure 7 is a cross section of the deformed crack mesh within the 2.5 inch radius cylinder, showing that the crack deformation is axisymmetric. The maximum distortion of the mesh is 5% on the $r = 0.5$ inch ring of nodes.

Figures 8 and 9 show plots of the deformed mesh, for the 2.5 inch and 4 inch radius cylinders, against plots of an ellipse. The figure shows that the crack deformation approximates an elliptical shape.

The close agreement between the theoretical and numerical results shown in Figures 6 through 9 indicates that the BRIDGE, BINTEQ, and DDID codes give accurate results for a three-dimensional problem involving a crack buried in a cylinder of finite radius and essentially infinite length.

From the theoretical solution for an infinitely long cylinder (4.1), and the numerical results illustrated in Figure 6, it is apparent that a cylinder with radius less than five times the crack radius must be treated as having a finite radius. To test the method in a finite body, cylinders of finite height and radius were analyzed. Cylinders of radius 2.5 and 4 inches were used in the test. Figure 10 shows a plot of the crack center displacement against cylinder half-height for a 4 inch radius cylinder. Figure 11 plots the same results for the 2.5 inch radius cylinder. Both show that the crack displacement increases as the cylinder height decreases. No theoretical solution was found to compare with the results but the behavior for both cylinders is qualitatively as expected. As the cylinder height decreases, the crack center displacement increases.

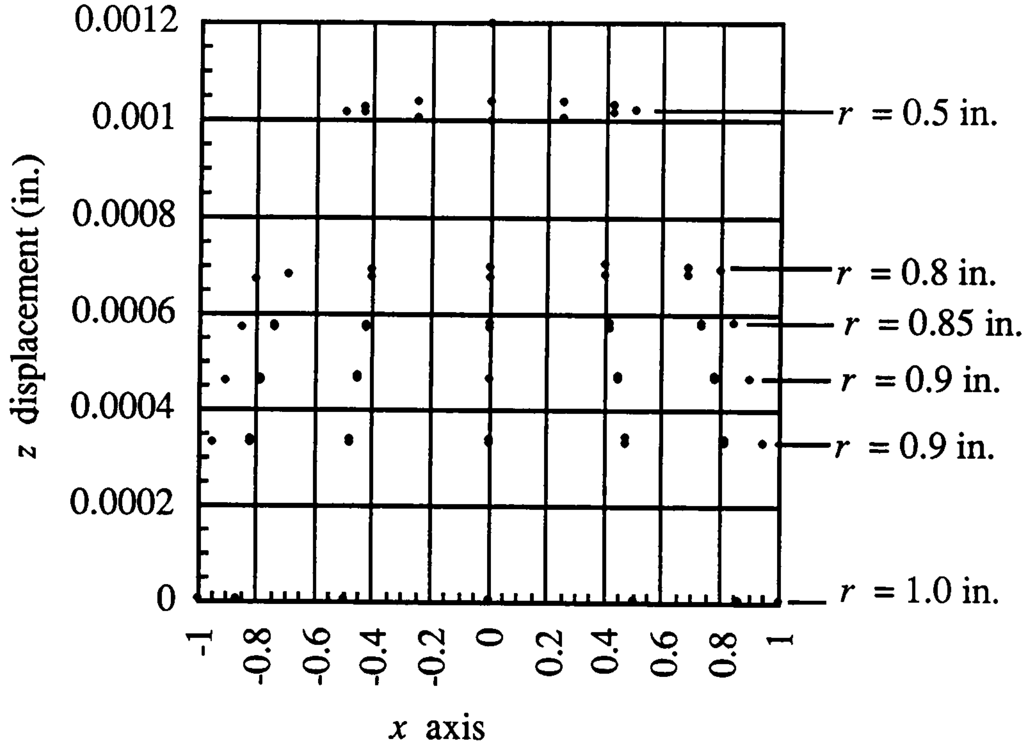

Figure 7. Deformed mesh for the r = 2.5 inch cylinder showing axisymmetry of results.

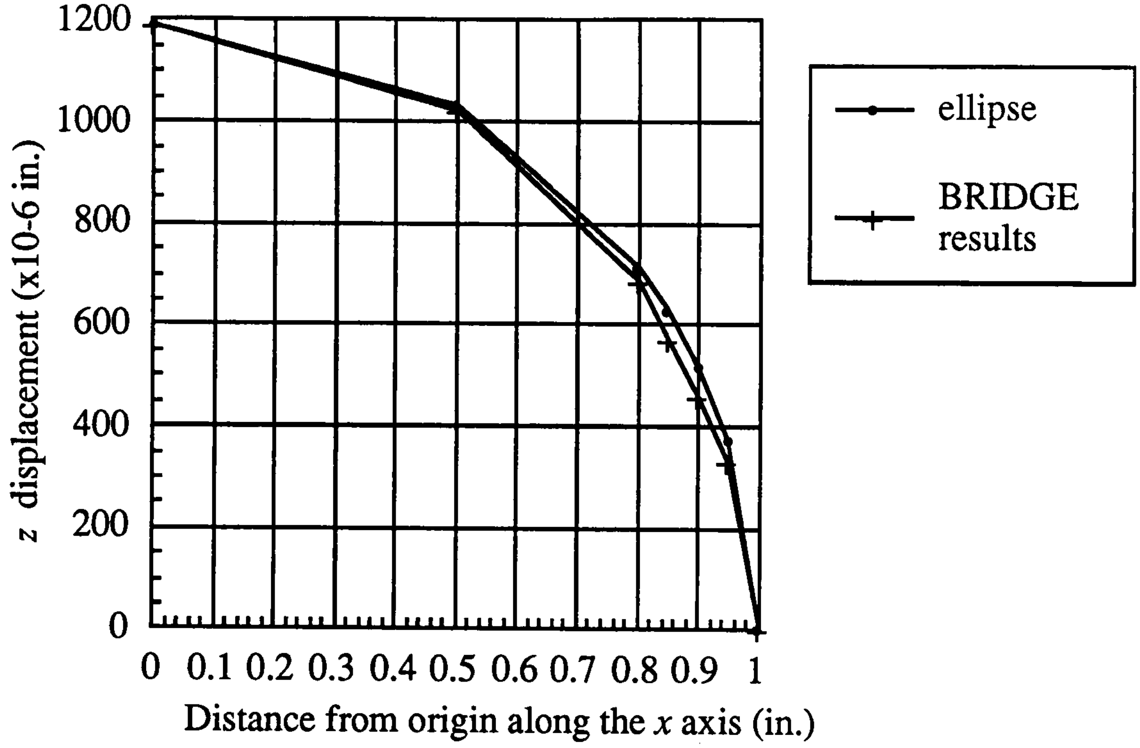

Figure 8. Comparison of BRIDGE results along a radius with an ellipse showing elliptical shape of the deformed crack inside a cylinder of radius 2.5 inch.

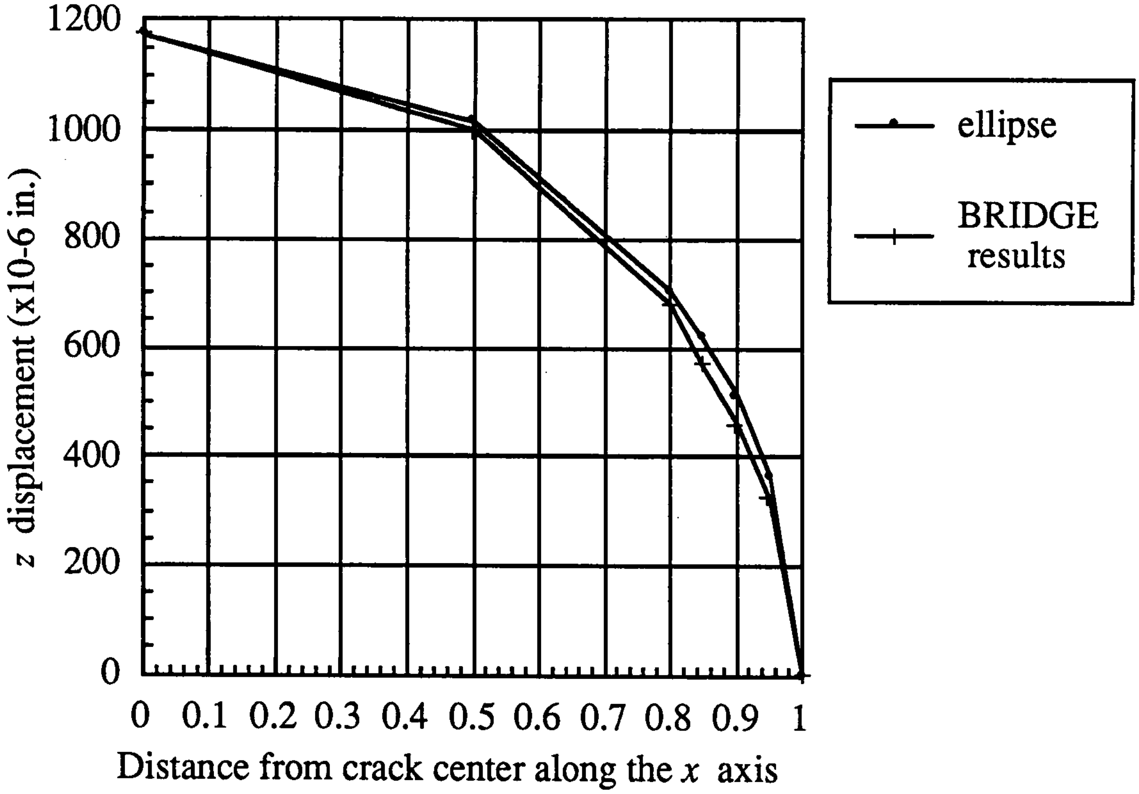

Figure 9. Plot of BRIDGE results along a radius with an ellipse showing elliptical behavior of a crack inside a cylinder of radius 4 inches.

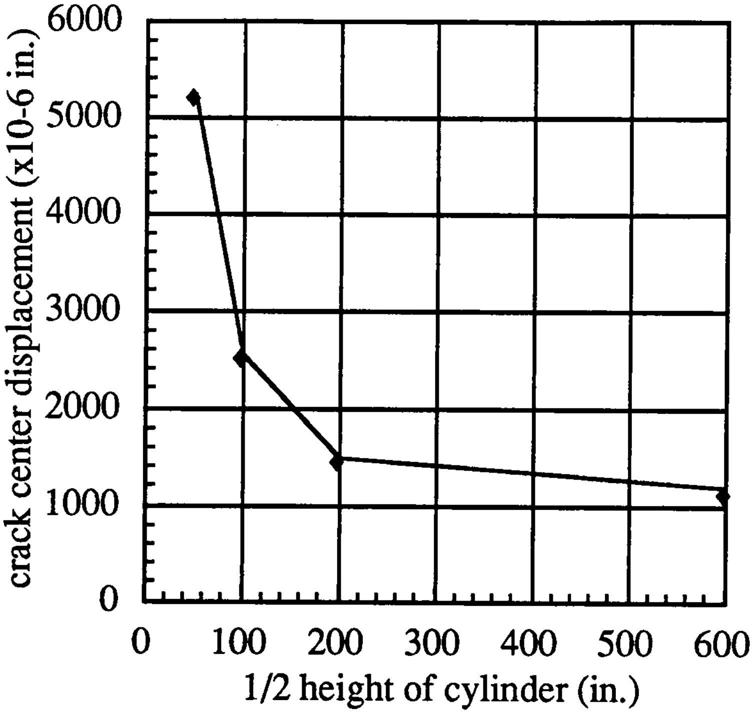

Figure 10. Comparison of crack center displacement vs. cylinder half-height for a 4 inch radius cylinder and a one inch radius crack.

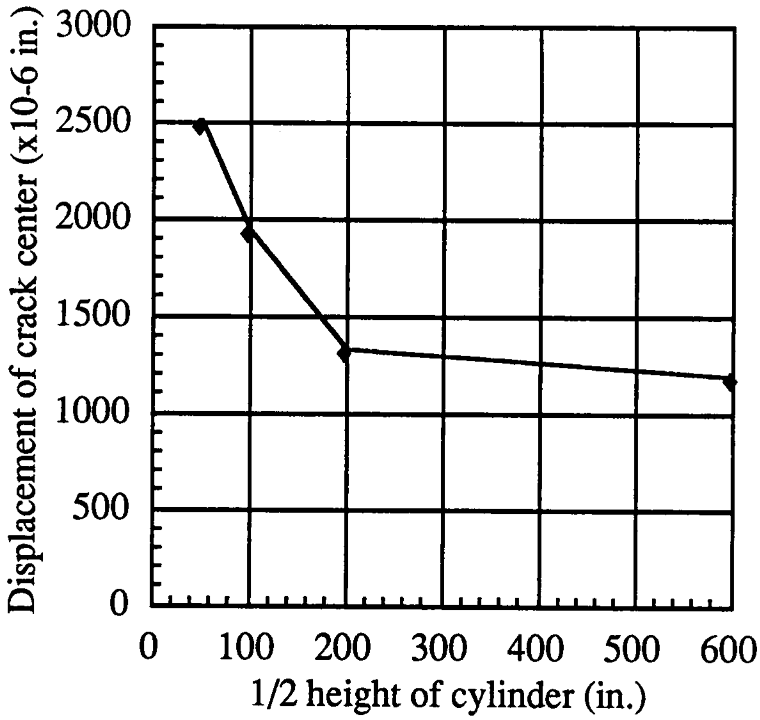

Figure 11. Comparison of crack center displacement vs. cylinder half-height for a 2.5 inch radius cylinder and one inch radius crack.

Figure 12 is a plot of the deformed mesh from the small cylinder showing that axisymmetry is still maintained although the distortion has increased. This illustrates a need for better control of round-off error.

Figure 13 shows that the crack behavior for the short cylinder of radius 2.5 inches is still elliptical although there is some distortion.

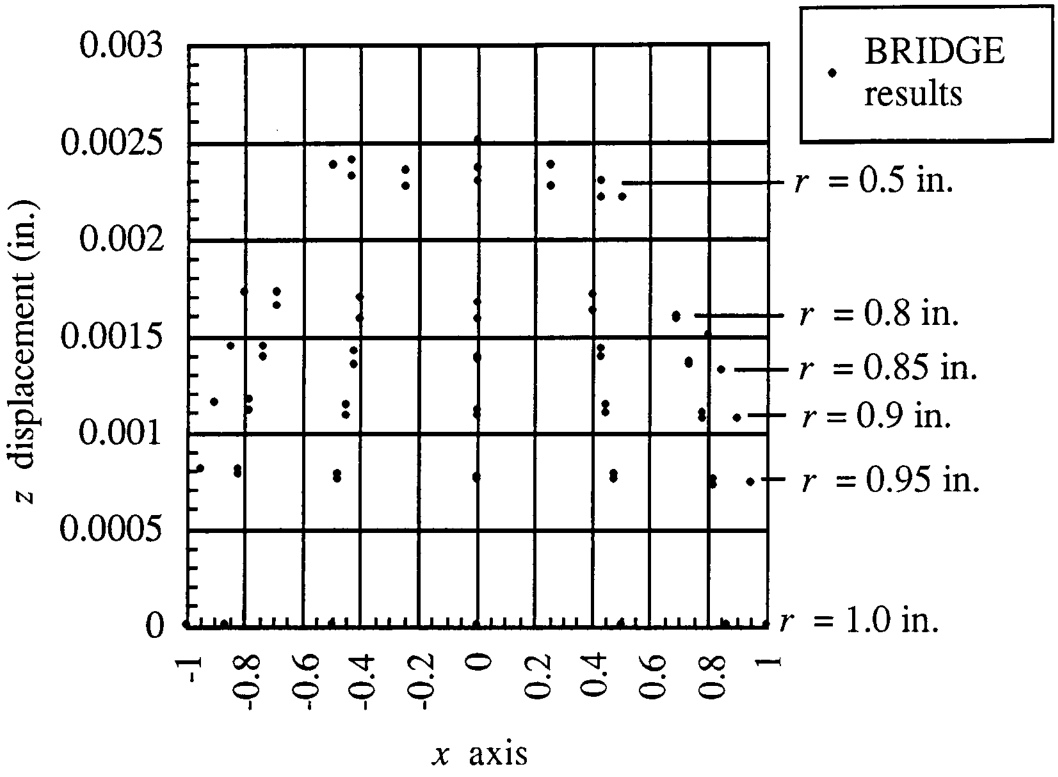

Figure 12. Plot of results for cylinder of 50 inch half-height and radius of 2.5 inches showing axisymmetry of results.

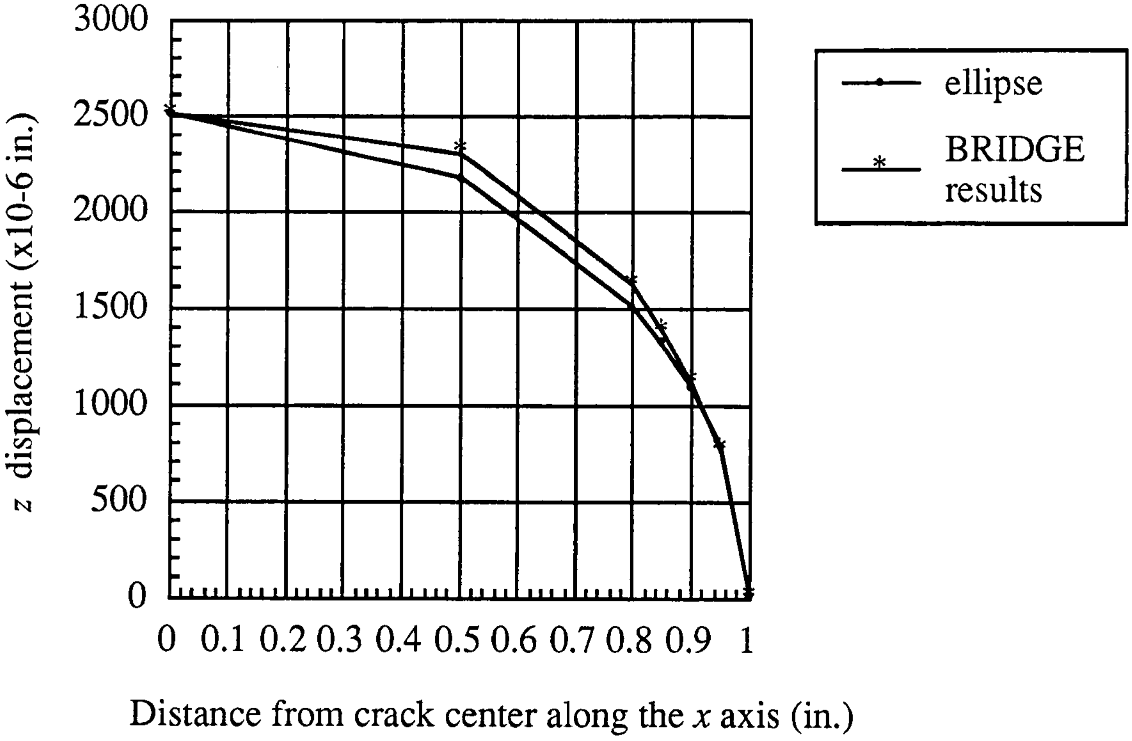

Figure 13. Comparison of BRIDGE results along a radius and ellipse showing elliptical behavior of a crack inside a cylinder of radius 2.5 inches.

CHAPTER 5

FUTURE WORK

In addition to modeling planar cracks, the method described herein has the capability of modeling non-planar cracks. Although DDID was written to be capable of handling such cases, it was not correctly working at the time of this research. If the code were fixed, the method presented would be capable of handling non-planar and multiple cracks. Cases where crack-face interference occurs could also be examined. In such a case, where inter-penetration of the crack surfaces occurs, a nodal traction can be applied to 'push' the surfaces back to the point where contact just occurs. The resulting surface tractions on the crack face are contained in the right-hand side vector of the system solved. A preliminary version of an iterator was developed for use with the DDID code. This iterator can be adapted for use with the BRIDGE code.

The stress intensity factors for cracks can be computed from the output of the crack simulation. One method of determining the stress intensity factor is to use the relation between the energy release rate and the stress intensity factor

$$G = \frac{K^2}{E} \tag{6.1}$$

where

G is the energy release rate,

K is the stress intensity factor, and

E is the elastic modulus.

The energy release rate is calculated by using a virtual crack extension as shown in two-dimensions by Figure 14. The region S_0 undergoes rigid body translation, and the material outside S_1 remain fixed. The energy release rate can be calculated from

$$G = \frac{1}{\Delta A_c} \int_V \left(\sigma_{ij} \frac{\partial u_j}{\partial x_k} - w\,\delta_{ik} \right) \frac{\partial \Delta x_k}{\partial x_i}\, dV - \frac{1}{\Delta A_c} \int_S T_i \frac{\partial u_i}{\partial x_j} \Delta x_j \, dS \quad (6.2)$$

where

ΔA_c is the increase in crack area generated by a virtual crack extension,

σ_{ij} is the stress state at the nodes,

w is the strain energy density,

u_i is the displacements of the nodes,

Δx_k is the displacement vector between S_0 and S_1 ,

V is the volume of the body,

S is the crack surface, and

T_i is the traction on the crack surface.

When extended to accommodate crack-face interference in non-planar cracks and to include calculation of stress intensity factors, the method described here would provide a basis for predicting fracture of objects made of brittle material and containing cracks with realistic geometry.

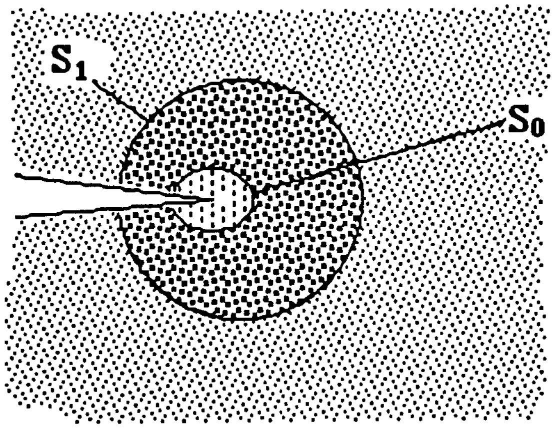

a. initial state

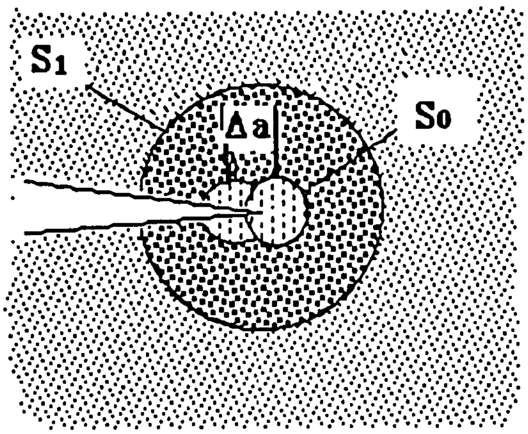

b. After virtual crack advance

Figure 14. Two-dimensional representation of a virtual crack extension (reproduced from Anderson, p. 673).

CHAPTER 6

CONCLUSIONS

A new BIE method for cracked, finite bodies has been formulated and implemented in a computer program. The method uses both Somigliana's displacement identity and a traction boundary integral equation. From the results shown above, the following conclusions were made.

1. The accuracy of the new BIE method has been verified for a circular crack in an infinitely long cylinder. The new method predicts crack opening displacement, crack ellipticity, and crack axisymmetry within 5% of the analytical solution.

2. It has been shown that the accuracy of new method can be improved by refining the boundary element mesh.

3. For cylinders of finite length, the variation of the crack opening with cylinder height is qualitatively correct. As the cylinder becomes smaller, the crack displacement discontinuities become larger.

4. The new method could be extended to the analysis of non-planar cracks and cases where crack-face interference occurs.

5. The new method could be extended to calculate stress intensity factors.

BIBLIOGRAPHY

BIBLIOGRAPHY

Anderson, T.L., Fracture Mechanics Fundamentals and Applications, CRC Press, Boston, 1991.

Brebbia, C.A., J.C.F. Telles, and L.C Wrobel, Boundary Element Techniques, Springer-Verlag, New York, 1984.

Cruse, T.A., "Numerical Solutions in Three Dimensional Elastostatics", *Int. J. Solids Struct.*, **5(12)**, pp. 1259-1274, 1968

Cruse, T.A. and W. Vanburen, "Three-Dimensional Elastic Stress Analysis of a Fracture with an Edge Crack", *Intl. J. of Fracture Mechanics*, **7**, pp. 1-15, 1971.

Cruse, T.A., "An Improved Boundary-Integral Equation Method For Three Dimensional Elastic Stress Analysis", *Int. J. Computers and Structures*, **4**, pp. 741-754, 1974.

Cruse, T.A. and G.J. Meyers, "Three-Dimensional Fracture Mechanics Analysis", *Journal of the Structural Division*, **103**, pp. 309-320, 1977.

Cruse, T.A., Boundary Element analysis in Computational Fracture Mechanics, Kluwer Academic Publishers, Boston, 1988.

Cruse, T.A. and G. Novati, "Traction BIE Formulations and Applications to Non-Planar and Multiple Cracks", presented at 22nd National Symposium on Fracture Mechanics, June 26-28, Atlanta, Georgia, 1990.

Lachat, J.C. and J.C. Watson, "Effective Treatment of Boundary Integral Equations: A Formulation for Three-Dimensional Elastostatics", *Intl. J. Structures,* **10**, pp. 991-1005, 1976.

Sneddon, I. N., Crack Problems in the Classical Theory of Elasticity, John Wiley & Sons, Inc., New York, 1969.

Tada, H., P. Paris, and G. Irwin, Stress Analysis of Cracks Handbook, Paris Productions, Inc., St. Louis, 1985.

APPENDIX

APPENDIX

The method described herein uses oblique coordinates for the integration. Any point in the triangle can be expressed as a function of the rectangular Cartesian coordinates of the vertices and the oblique coordinates using

$$x_i = x_i^j \eta_j$$

where

x_i are the coordinates of the point,

x_i^j are the coordinates of the triangle vertices, and

η_i are the oblique coordinates of the point.

Because the oblique coordinates vary from 0 to 1 along each element side and linear interpolation is used for the integration, the oblique coordinates are also the interpolation functions. The interpolation functions can be written in terms of rectangular Cartesian coordinates by

$$\eta_1 = \frac{1}{2A}\left(2A_1^0 + b_1 x_1 + a_1 x_2\right),$$

$$\eta_2 = \frac{1}{2A}\left(2A_2^0 + b_2 x_1 + a_2 x_2\right), \text{ and}$$

$$\eta_3 = 1 - \eta_1 - \eta_2$$

where

A is the area of the triangle,

$a_i = x_i^k - x_i^j$,

$b_i = x_2^j - x_2^k$, and

$2A_i^0 = x_1^j x_2^k - x_1^k x_2^j$.

For the above equations, the indices follow the pattern

$$i = 1, j = 2, k = 3$$
$$i = 2, j = 3, k = 1$$
$$i = 3, j = 1, k = 2$$

Alternately, the interpolation functions can be written as

$$\eta_i = \frac{A_i}{A}$$

where

A_i is the area of a triangle formed by the point of interest and the other two triangle vertices (see Figure)

A is the area of the element.

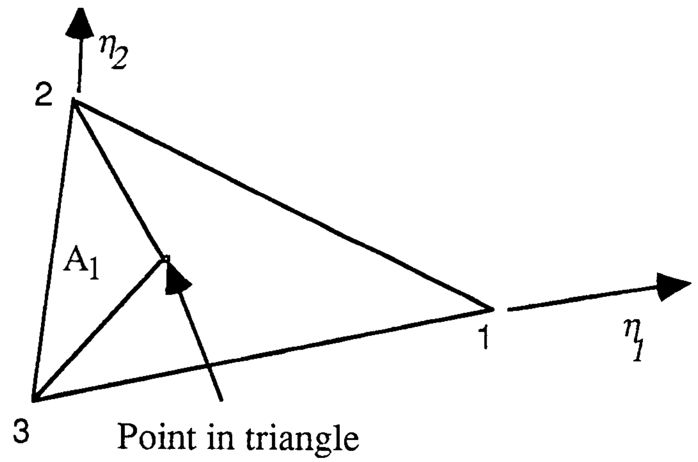

Geometric representation of η_1 for a general triangular element.

Vita

G. Russell McNutt was born in Knoxville, Tennessee on January 25, 1968. He attended school in the Knoxville area and graduated from Doyle High School in June, 1986. The following September, he entered The University of Tennessee and in December, 1990 received a Bachelor of Science in Engineering Science. He reentered The University of Tennessee in January, 1991 and in December, 1992 received a Master of Science in Engineering Science.